FOURTEENTH EUROPEAN ROTORCRAFT FORUM

Paper No. 69

SYSTEM IDENTIFICATION STRATEGIES FOR HELICOPTER ROTOR MODELS INCORPORATING INDUCED FLOW

C G Black[+]

R Bradley[+]

D J Murray-Smith[*]

Department of Aerospace Engineering [+]

and

Department of Electronics and Electrical Engineering[*]
University of Glasgow
U.K.

20 - 23 September, 1988

MILANO ITALY

ASSOCIAZIONE INDUSTRIE AEROSPAZIALI
ASSOCIAZIONE ITALIANA DI AERONAUTICA ED ASTRONAUTICA

SYSTEM IDENTIFICATION STRATEGIES FOR HELICOPTER ROTOR MODELS INCORPORATING INDUCED FLOW

C.G. Black, R. Bradley, D.J. Murray-Smith

University of Glasgow

ABSTRACT

The effect of dynamics of induced flow through the main rotor is often cited as a cause of control-power deficiency relative to that predicted by simple simulation models of the type which are at present widely used in the design of flight control systems for helicopters. In addition, rotor dynamics themselves pose bandwidth restraint problems for control system design. The validation of models incorporating rotor dynamics and induced flow dynamics is therefore of considerable importance. System identification techniques provide one approach to the development and validation of improved rotor models. This paper presents a general methodology for the identification of rotor models, principally based upon frequency-domain output-error methods. Strategies are presented involving a number of different forms of model structure involving induced-flow models based on either momentum or vortex theory. Preliminary results are presented for flight data provided by RAE (Bedford) which involve kinematic and flapping data of high quality. An assessment is made of the value of the available identification tools and some conclusions are reached concerning the importance of induced-flow effects for the flight data sets used.

NOMENCLATURE

A	System matrix of rotor
B	Effective control matrix for state-space representations
C	Coefficient matrix of $\underline{\beta}'$ in flapping equation
D	Coefficient matrix of $\underline{\beta}$ in flapping equation
E	Coefficient matrix of $\underline{x}'$ in modified state equation
H	Measurement matrix
τ	Induced-flow time constant
$\underline{\beta}$	Vector of harmonic components of flapping
H_λ	Coefficient matrix for $\underline{\lambda}$ in flapping equation

H_θ Coefficient matrix for $\underline{\theta}$ in flapping equation

H_η Coefficient matrix for $\underline{\eta}$ in flapping equation

F_β Coefficient matrix for $\underline{\beta}$ in non-dimensional dynamic induced-flow equation

$F_{\beta'}$ Coefficient matrix for $\underline{\beta}'$ in non-dimensional dynamic induced-flow equation

F_θ Coefficient matrix for $\underline{\theta}$ in non-dimensional dynamic induced-flow equation

F_η Coefficient matrix for $\underline{\eta}$ in non-dimensional dynamic induced-flow equation

F_ν Coefficient matrix for $\underline{\nu}$ in non-dimensional induced-flow equation

$\underline{x}$ State vector

$\underline{u}$ Control vector

$\underline{\theta}$ Vector of harmonic components of blade pitch

$\underline{\lambda}$ Vector of harmonic components of non-dimensional induced-flow

$\underline{\eta}$ Vector of non-dimensional pitch and roll accelerations

$\underline{\nu}$ Vector of non-dimensional inflow due to hub motion

$\underline{z}$ Measurement vector

J Cost function

$\underline{\epsilon}$ Error vector

S Error covariance matrix

1. INTRODUCTION

The increasing demand for agility in the modern helicopter and the need for precise manoeuvres has focussed attention upon the control power available to the pilot and on the possible sources of observed deficiency in control power relative to that predicted by the currently available simulation models. The dynamics of induced flow through the rotor are often cited as a cause of transient control-power deficiency and this gives a standpoint from which to assess current models of induced flow, such as that based on local momentum theory. In turn, these models should be validated against flight data using proven techniques within a methodology appropriate to the context.

System identification techniques, which have been applied successfully to the estimation of parameters of six-degree-of-freedom, rigid-body helicopter models, provide one possible means of developing and validating improved models of helicopters and of investigating induced-flow phenomena. One approach to system identification which has been developed during recent studies at the University of Glasgow[1,2,3] combines equation-error and output-error methods in the frequency domain. Although originally

developed for the identification of six-degrees-of-freedom models, this approach is also well suited to the investigation of rotor models since it allows flight data outside the frequency range of interest to be excluded from the analysis and thus permits models to be established which are valid over a defined frequency range. This provides a means of partially decoupling the task of estimating parameters of a rotor model, which involves relatively high frequencies, from the identification of the lower-frequency, rigid-body dynamics of the helicopter.

In the case of rotor models which incorporate induced-flow dynamics, equation-error identification methods cannot be applied since the inflow variable cannot be measured directly. In such cases, output-error methods must be adopted for the identification of parametric models.

2. THEORETICAL MODELS INCORPORATING INDUCED FLOW

An outline derivation of the theoretical models upon which the subsequent system identification is based may be found in the Appendix. The most general form of the model considered involves equations of second order, and these may be readily reduced to a first-order form with induced-flow dynamics or to a first or second order form without inflow dynamics. The general model and these associated reduced forms, are of considerable potential value for the study of inflow phenomena using system identification and parameter-estimation techniques.

2.1 Second-Order Form with Induced-Flow Dynamics

As shown in the Appendix the second-order form of model is as follows:

$$\begin{bmatrix} I & 0 & 0 \\ 0 & I & 0 \\ 0 & 0 & \text{diag } \tau \end{bmatrix} \begin{bmatrix} \underline{\beta} \\ \underline{\beta}' \\ \underline{\lambda} \end{bmatrix}' = \begin{bmatrix} 0 & I & 0 \\ -D & -C & H_\lambda \\ F_\beta & F_{\beta'} & (F_\lambda - I) \end{bmatrix} \begin{bmatrix} \underline{\beta} \\ \underline{\beta}' \\ \underline{\lambda} \end{bmatrix} + \begin{bmatrix} 0 & 0 & 0 \\ H_\theta & H_\nu & H_\eta \\ F_\theta & F_\nu & 0 \end{bmatrix} \begin{bmatrix} \underline{\theta} \\ \underline{\nu} \\ \underline{\eta} \end{bmatrix} \qquad (1)$$

where all the vectors and matrices are as defined in the Appendix. Premultiplying both sides of equation 1 by the inverse of the matrix on the left gives a model in the standard state space form.

$$\underline{x}' = A\underline{x} + B\underline{u} \tag{2}$$

The elements of the system matrix A and distribution matrix B of equation 2 are functions, in some cases of a relatively complicated form, of the physical parameters which appear as elements of the matrices of equation 1.

2.2 First Order Form with Induced-Flow Dynamics

By neglecting second-derivative terms in the flapping equation, the second-order model above may be reduced to a set of first-order equations of the following form

$$\begin{bmatrix} C & 0 \\ -F_{\beta}' & \text{diag } \tau \end{bmatrix} \begin{bmatrix} \underline{\beta} \\ \underline{\lambda} \end{bmatrix}' = \begin{bmatrix} -D & H_{\lambda} \\ F_{\beta} & (F_{\lambda} - I) \end{bmatrix} \begin{bmatrix} \underline{\beta} \\ \underline{\lambda} \end{bmatrix}$$

$$+ \begin{bmatrix} H_{\theta} & H_{\nu} & H_{\eta} \\ F_{\theta} & F_{\nu} & 0 \end{bmatrix} \begin{bmatrix} \underline{\theta} \\ \underline{\nu} \\ \underline{\eta} \end{bmatrix} \tag{3}$$

As with equation 1 this matrix equation may be manipulated into the standard state-space form.

2.3 Second-Order Form without Induced-Flow Dynamics

If the time constants associated with the induced flow are negligible the general second-order equation of Section 2.1 reduces to the following form:

$$\begin{bmatrix} \underline{\beta} \\ \underline{\beta}' \end{bmatrix}' = \begin{bmatrix} 0 & I \\ -D & -C \end{bmatrix} \begin{bmatrix} \underline{\beta} \\ \underline{\beta}' \end{bmatrix} + \begin{bmatrix} 0 & 0 & 0 & 0 \\ H_{\theta} & H_{\nu} & H_{\lambda} & H_{\eta} \end{bmatrix} \begin{bmatrix} \underline{\theta} \\ \underline{\nu} \\ \underline{\lambda} \\ \underline{\eta} \end{bmatrix} \tag{4}$$

Equation 4 is in standard state-space form.

2.4 First-Order Form without Induced-Flow Dynamics

From equation 3, if the time constants associated with the induced flow are neglected, we obtain the following equation

$$C\underline{\beta}' = -D\underline{\beta} + H_{\theta}\underline{\theta} + H_{\nu}\underline{\nu} + H_{\lambda}\underline{\lambda} + H_{\eta}\underline{\eta} \tag{5}$$

As with the models of Sections 2.1 and 2.2, this equation can be readily expressed in state–space form by premultiplying throughout by the inverse of the matrix C.

3. IDENTIFICATION OF ROTOR MODELS

An identification methodology, based upon the use of frequency–domain techniques, has been developed at the University of Glasgow and has been applied with success to the identification of rigid body models of helicopters[1,2,3]. The approach used involves three distinct stages. The first of these is a frequency–domain equation–error identification to provide initial estimates for use in subsequent stages of the process. This equation–error stage also provides information of relevance in the selection of the most suitable model structure. The second stage involves the application of a frequency–domain output–error method which can provide unbiased model parameter estimates in the absence of process noise. The final step in this three–stage process uses a time–domain output–error approach to estimate bias terms and offsets and to provide a time–domain verification of the model identified in the frequency domain.

There are a number of advantages in using the frequency domain for rotorcraft system–identification. The most notable of these is the ability to define a frequency range over which the estimation is to be carried out and for which the identified model is valid. The use of frequency–domain data can also facilitate the computation of parameter estimates because of the significant reduction in the amount of data when a restricted frequency range is used. Modelling features such as time delays can also be accommodated readily using a frequency–domain approach.

The discussion of model structures in Section 2 has shown that the standard state–space description is not always the most appropriate form for rotor models. A modified form of state equation can facilitate the direct estimation of physical parameters. The modified state equation can be written as

$$E\underline{x}' = A\underline{x} + B\underline{u} \qquad (6)$$

In general, clearly defined relationships can exist between elements of the A, B and E matrices. The identification software developed at the University of Glasgow allows relationships between different parts of the model structure to be incorporated as constraints in the identification for the frequency–domain output–error method. This feature is very useful when the elements of the model are functions of a few parameters only. For example, the first–order model given by equation 3 requires the direct estimation of the three parameters: λ_β^2, n_β, and τ (see Appendix). Three elements in the model are chosen to be used to identify these parameters, and the sensitivity information and values of all other elements in the model are derived using the defined

relationships and estimated values of these parameters.

The measured quantities $\underline{z}$ are related to states in the model $\underline{x}$ through the equation:

$$\underline{z} = H\underline{x} + \underline{v} \tag{7}$$

where $\underline{v}$ is assumed to be a band-limited white-noise source. It is assumed that the frequency range used in the identification is equal to, or lies within the band limit of the white noise, if unbiased model parameter estimates are to be obtained.

The cost-function minimised for the output-error identification has the form:

$$J = \sum_{\omega_1}^{\omega_2} \left[\underline{\epsilon}^* S^{-1} \underline{\epsilon} + \log_e |S| \right] \tag{8}$$

where $\underline{\epsilon}$ represents the difference between the observations and the model output in the frequency domain. S is the error-covariance matrix and $[\omega_1, \omega_2]$ represents the range of frequencies used in the identification. For the current estimation problem, where induced-flow states (λ_0, λ_{1C}, λ_{1S}) are present in the model given by equation 7 but for which no related measurements are provided for in equation 8, the diagonal elements of the error-covariance matrix S associated with inflow are fixed at very large (effectively infinite) values. The other diagonal elements of the error-covariance matrix are estimated in addition to the model parameters present in equations 7 and 8, and convergence is required in both sets of parameters before the identification algorithm is terminated.

A distinct advantage of the frequency-domain approach is the ability to use a restricted frequency range in the identification. The frequency range selected by the analyst is that which is deemed appropriate for the model in question. The minimisation of the output-error cost function given in equation 8 is carried out using Fourier-transformed quantities obtained for the stipulated frequency range.

3.1 Selection of Frequency Range

For the current problem, an upper limit of about 1.6 Hz was arrived at from the equation-error approach by fixing the lower frequency value and examining the effect on the confidence of individual parameter estimates (partial-F statistics) and on the squared-correlation coefficient (R^2 - indicating the goodness of the fit) as the upper frequency was varied. It can be seen from Figure 1 that the magnitudes of the transforms are very small in the region around 1.6 Hz. Peaks in the spectra do exist at

higher frequencies but these are associated with once-per-revolution effects and contain no useful information for the identification. A similar approach was used in establishing the lower frequency value of 0.226 Hz. used in the identification.

Output-error results, where the lower frequency value is varied upwards from the smallest available frequency, also suggest that a lower frequency of 0.226 Hz, is appropriate for the identification. It is found that the error-bounds in all of the parameters decrease as the lower frequency bound is increased up to 0.226 Hz. The use of the next available frequency point: 0.263 Hz - corresponding to a rigid-body mode in the discrete spectrum - resulted in the algorithm failing to converge. The use of an even higher low-frequency limit would imply the exclusion of rigid-body coupling from the rotor models.

3.2 Model Structures Involving No Inflow Dynamics

The first approach used here for the identification of a rotor model involved a state-space model of the form given by equation 2. No induced-flow dynamics were incorporated, and the states in the model were the multiblade quantities β_0, β_{1C} and β_{1S} obtained using a multiblade transformation on individual blade measurements.

Equation-error and output-error techniques were used to obtain estimates of elements of the state and control matrices, a_{ij} and b_{ij} respectively for a Puma helicopter flying at 100 knots. A longitudinal-cyclic doublet input was applied by the pilot during the run. A comparison of the estimates obtained, with approximate theoretical (quasi-static induced flow) values predicted by the HELISTAB simulation model[4] is shown in Table 1 for the most significant model parameters.

Two features are worthwhile pointing out from Table 1: firstly, that a better agreement with theory is obtained for the frequency range 0.213-1.60 Hz. than by using all the available frequencies in the identification - the selection of an appropriate frequency range will be discussed below - and, secondly, further improvement is obtained in using the output error rather than equation-error identification technique.

The elements of the matrices in the standard state-space form used in the identification described above are, as was described earlier, functions of the physical parameters λ_β^2 and n_β. For this reason, it was felt that a more satisfactory approach to the rotor modelling would be to try to estimate these parameters directly. This involved modifying the identification software so that a state-space model of the form given by equation 6 could be used. The clearly defined relationships existing between elements of the E, A and B matrices were also to be incorporated into the identification.

The natural formulation of the first or second-order models, with or without induced flow can be expressed in the form given by equation 6.

The general formulation given by equation 1 involves second-order flapping dynamics. It was found that the results obtained for the use of first and second-order models were almost identical. This provided some justification for using models with only first-order flapping and inflow dynamics in the subsequent work. It is worthwhile noting that the first and second-order formulations have the same number of unknown parameters, but the dimensions of the matrices in the model are different.

Using the output-error method for a first-order model without inflow dynamics, as given by equation 5, estimates were obtained for the physical parameters λ_β^2 and n_β; these are shown in Table 2 along with the theoretical values. The estimate of λ_β^2 is larger than would be expected from theory, whilst the n_β estimate compares well with theory.

3.3 Model Structures with Induced-Flow Dynamics

The next step in the investigation was to use induced-flow dynamics in the identification with the model structure given by equation 3. Induced-flow states were not, of course, measured and the technique described earlier of fixing the elements of the error-covariance matrix corresponding to the induced-flow states to very high values, effectively blocking out any measurement information from the identification, was employed. With the induced-flow model incorporated, an additional parameter, namely the time constant for the induced flow, was also estimated. For the results presented in Table 3, both momentum-theory and vortex-theory induced-flow models were used.

It would be difficult to reach any conclusions at this stage about the two sets of results other than to say that momentum and vortex results show some differences. A time constant of about 0.3 seconds (when converted from -8.22 in non-dimensional time Ωt) is obtained for the momentum-inflow model. For the vortex-inflow model the time constant is overwhelmed by its accompanying error bound and may be taken as an approximation to zero. The incorporation of induced-flow dynamics does appear to have had some effect on the estimates of the physical parameters, most notably n_β. (Tables 2 and 3). It is of interest to note that other investigators have used more complex models[7] and report larger time constants in the induced flow dynamics.

Consider first the momentum-inflow results. The estimates of some of the elements of the matrices for a state-space formulation of the type given by equation 2 (considered earlier in the context of the direct identification of these non-physical parameters)

constructed from the physical parameter values, are shown in Table 4. In addition to the results corresponding to the incorporation of a momentum-inflow model, the corresponding values obtained from a first-order model without induced-flow are shown for comparison. The incorporation of a momentum-inflow model appears to have little effect on the values of most of the estimates, confirming the view that at this flight condition the induced flow has a minor influence in physical terms.

Frequency-domain fits (magnitude and phase) for the cases without and with a momentum-inflow model are shown in Figures 1 and 2. A significantly better agreement between measurement and prediction is obtained at the lowest frequency used in the identification when the momentum-inflow model is used in comparison to the situation when no inflow is modelled.

A good match between measured and predicted values is obtained for the magnitude and phase of β_{1C}. This is also brought out in the time-domain reconstruction of the frequency-domain identified models shown in Figure 3. However, the corresponding fits for β_{1S} and β_O in both the frequency and time domains reveal that there is still some deficiency in the model as it stands. The oscillations present in the measurements of β_O and β_{1S} correspond to peaks in the frequency-domain magnitude spectrum which the identified model is unable to account for.

4. CONCLUSIONS AND RECOMMENDATIONS

This paper describes a successful application of established parameter estimation tools to helicopter rotor models within a system identification strategy. An early consequence of the work was that it provided motivation for the further development of those tools so that they could make use of a more general formulation of the equations in which the physical parameters of the model occur in a simple way. This provides a release from the restrictions of the state-space representation where these parameters can feature in a complex and intractible manner. In addition a successful technique was devised for including unmeasured states in a parameter estimation method.

It is clear from the results obtained that the second derivative term can be dropped from the flapping equation expressed in multiblade coordinates. The reduced order system that remains gives virtually unchanged estimates for the physical parameters of the model. Although it can be demonstrated theoretically that such a reduction of order leaves the dominant mode of the system virtually unchanged, the value of this model is often doubted, and the confirmation from flight data is worth noting.

The value of reducing the order of the induced-flow equation by dropping the

derivative term is not so clear since the flight condition for the given data is not one for which induced flow would be expected to have a major influence on the rotor dynamics. Indeed the values of the estimates of the rotor parameters are little influenced by the choice of model for the induced flow. What evidence there is shows that, for the models used in the present study, the dynamics of the induced flow are much faster than those of the dominant modes of the flapping equation, so that the reduced order equation is a good approximation.

Future work should continue the basic strategy and investigate flight conditions, where induced flow is considered to be more significant. Alternative models for the induced flow can be evaluated within the same strategy, for example a model appropriate to the hover condition is easily accommodated.

APPENDIX

1. Flapping Equation

The model structures for the blade dynamics are taken from the model described by Padfield[4]. The flapping equation may be written, in the absence of blade twist,

$$\underline{\beta}'' + C\underline{\beta}' + D\underline{\beta} = H_\theta\underline{\theta} + H_\nu\underline{\nu} + H_\lambda\underline{\lambda} + H_\eta\underline{\eta} \qquad \text{A1}$$

where $\underline{\beta} = (\beta_0, \beta_{1C}, \beta_{1S})^T$ are the flapping components of the multiblade representation.

$\underline{\theta} = (\theta_0, \theta_{1CW}, \theta_{1SW})^T$ are collective, lateral and longitudinal components of the blade pitch respectivelyin hub wind axes.

$\underline{\nu} = (\mu_z, \bar{q}_w, \bar{p}_w)^T$ are the non-dimensional quantities: component of rotor hub velocity normal to the rotor plane, pitch and roll rates of the rotor in hub wind axes.

$\underline{\lambda} = (\lambda_0, \lambda_{1C}, \lambda_{1S})^T$ are the mean and harmonic components of the induced flow.

$\underline{\eta} = (q'_w, p'_w)^T$ are the non-dimensional pitch and roll accelerations.

The matrices occurring in A1 are the following:

$$C = \begin{bmatrix} n_\beta & 0 & \frac{2}{3}\mu n_\beta \\ 0 & n_\beta & 2 \\ \frac{4}{3}\mu n_\beta & -2 & n_\beta \end{bmatrix} \qquad D = \begin{bmatrix} \lambda_\beta^2 & 0 & 0 \\ \frac{4}{3}\mu n_\beta & \lambda_\beta^2 - 1 & n_\beta\left[1+\frac{\mu^2}{2}\right] \\ 0 & -n_\beta\left[1-\frac{\mu^2}{2}\right] & \lambda_\beta^2 - 1 \end{bmatrix}$$

$$H_\theta = \begin{bmatrix} n_\beta[1+\mu^2] & 0 & \frac{4}{3}\mu n_\beta \\ 0 & n_\beta\left[1+\frac{\mu^2}{2}\right] & 0 \\ \frac{8}{3}\mu n_\beta & 0 & n_\beta\left[1+\frac{3\mu^2}{2}\right] \end{bmatrix} \qquad H_\eta = \begin{bmatrix} 0 & 0 \\ 1 & 0 \\ 0 & 1 \end{bmatrix}$$

$$H_\nu = \begin{bmatrix} \frac{4}{3} n_\beta & 0 & \frac{2}{3}\mu n_\beta \\ 0 & n_\beta & 2 \\ 2\mu n_\beta & -2 & n_\beta \end{bmatrix}$$

$$H_\lambda = \begin{bmatrix} -\frac{4}{3} n_\beta & 0 & -\frac{2}{3}\mu n_\beta \\ 0 & -n_\beta & 0 \\ -2\mu n_\beta & 0 & -n_\beta \end{bmatrix}$$

The matrices depend on the fundamental parameters λ_β, the normalised flapping frequency, and n_β, the inertia number. The non-dimensional component of hub velocity in the plane of the rotor, μ also occurs, but in the absence of perturbations in μ the equation A1 is linear and may be used for perturbations in $\underline{\beta}$, $\underline{\theta}$, $\underline{\nu}$, $\underline{\lambda}$, $\underline{\eta}$.

In a state-space representation of the reduced-order model the matrix $C^{-1}D$ is required.

$$C^{-1}D = \frac{1}{n_\beta\left[\left[n_\beta^2 + 4\right] - \frac{8}{9}\mu^2 n_\beta^2\right]} \begin{bmatrix} g_{11} & g_{12} & g_{13} \\ g_{21} & g_{22} & g_{23} \\ g_{31} & g_{32} & g_{33} \end{bmatrix}$$

where $g_{11} = \lambda_\beta^2 (n_\beta^2 + 4) - \frac{16}{9} \mu^2 n_\beta^2$

$g_{12} = -\frac{4}{3} \mu n_\beta (\lambda_\beta^2 - 1) + \frac{2}{3} \mu n_\beta^3 (1 - \frac{\mu^2}{2})$

$g_{13} = -\frac{4}{3} \mu n_\beta^2 (1 + \frac{\mu^2}{2}) - \frac{2}{3} \mu n_\beta^2 (\lambda_\beta^2 - 1)$

$g_{21} = \lambda_\beta^2 \frac{8}{3} \mu n_\beta + \frac{4}{3} \mu n_\beta^3 - \frac{32}{27} \mu^2 n_\beta^2$

$g_{22} = (n_\beta^2 - \frac{8}{9} \mu n_\beta)(\lambda_\beta^2 - 1) + 2n_\beta^2 (1 - \frac{\mu^2}{2})$

$g_{23} = (n_\beta^3 - \frac{8}{9} \mu n_\beta^2)(1 + \frac{\mu^2}{2}) - 2n_\beta (\lambda_\beta^2 - 1)$

$g_{31} = -\lambda_\beta^2 \frac{4}{3} \mu n_\beta^2 + \frac{8}{3} \mu n_\beta^2$

$g_{32} = 2n_\beta (\lambda_\beta^2 - 1) - n_\beta^3 (1 - \frac{\mu^2}{2})$

$g_{33} = 2n_\beta^2 (1 + \frac{\mu^2}{2}) + n_\beta^2 (\lambda_\beta^2 - 1)$

in which the parameters n_β and λ_β occur in a complex manner.

2. Induced Flow

The basic model for the induced flow takes the form

$$\underline{\lambda} = L\underline{c} \qquad \text{A2}$$

where $\underline{c}$ is a non-dimensional aerodynamic force and moment vector

$$\underline{c} = (C_T/a_o s \ , \ C_{mc}/a_o s \ , \ C_{ms}/a_o s)$$

The normalised rotor thrust is C_T while C_{mc} and C_{ms} are the normalised moments about the rotor y and x axes respectively. The rotor solidity is s, and the lift slope of the blade is a_o.

The matrix L is determined by the type of model used. The following choices are based on the derivation of Ormiston and Peters[5].

(i)
$$L_M = \begin{bmatrix} a_o s/2\mu & 0 & 0 \\ 0 & -a_o s/\mu & 0 \\ 0 & 0 & -a_o s/\mu \end{bmatrix} \qquad \text{A3}$$

is based on local momentum theory

(ii)
$$L_V = \begin{bmatrix} a_o s/2\mu & 0 & 0 \\ 2a_o s/3\mu & 0 & 0 \\ 0 & 0 & -2a_o s/\mu \end{bmatrix} \qquad \text{A4}$$

is an alternative based on the representation of the rotor as an equivalent vortex.

The dynamics of the induced flow can be incorporated in the manner suggested by several authors; for example Johnson[6]

$$\tau \underline{\lambda}' + \underline{\lambda} = L\, \underline{c} \qquad \text{A5}$$

where τ is a time constant.

3. Aerodynamic Force and Moments

The aerodynamic force and moments can be deduced from the work leading up to equation A1.

$$\underline{c} = C_{\beta'}\, \underline{\beta}' + C_{\beta}\underline{\beta} + C_{\theta}\underline{\theta} + C_{\nu}\underline{\nu} + C_{\lambda}\underline{\lambda} \qquad \text{A6}$$

where
$$C_{\beta'} = \begin{bmatrix} -\frac{1}{6} & 0 & -\mu/8 \\ 0 & \frac{1}{16} & 0 \\ \frac{\mu}{12} & 0 & 1/16 \end{bmatrix}$$

$$C_{\beta} = \begin{bmatrix} 0 & 0 & 0 \\ \frac{\mu}{12} & 0 & \frac{1}{16}\left(1+\frac{\mu^2}{2}\right) \\ 0 & -\frac{1}{16}\left(1-\frac{\mu^2}{2}\right) & 0 \end{bmatrix}$$

$$G_\theta = \begin{bmatrix} \left[\frac{1+\mu^2}{6}\frac{}{4}\right] & 0 & \frac{\mu}{4} \\ 0 & -\frac{1}{16}\frac{(1+\mu^2)}{2} & 0 \\ \frac{-1}{6} & 0 & -\frac{1}{16}\frac{(1+3\mu^2)}{2} \end{bmatrix}$$

$$G_\nu = \begin{bmatrix} \frac{1}{4} & 0 & \frac{\mu}{8} \\ 0 & -\frac{1}{16} & 0 \\ -\frac{\mu}{8} & 0 & \frac{-1}{16} \end{bmatrix}$$

$$G_\lambda = \begin{bmatrix} \frac{-1}{4} & 0 & -\frac{\mu}{8} \\ 0 & \frac{1}{16} & 0 \\ \frac{\mu}{8} & 0 & \frac{1}{16} \end{bmatrix}$$

4. Eliminations

For an instantaneously-adjusting induced flow τ can be set to zero in A5 and A6 used to eliminate $\underline{\lambda}$ from A1, which then becomes

$$\underline{\beta}'' + C^* \underline{\beta}' + D^* \underline{\beta} = H_\theta{}^* \underline{\theta} + H_\nu{}^* \underline{\nu} + H_\eta \underline{\eta} \qquad \text{A7}$$

where

$C^* = C - H_\lambda[I - LG_\lambda]^{-1} L G_{\beta'}$, and similarly for D^*

and

$H_\theta{}^* = H_\theta + H_\lambda[I - LG_\lambda]^{-1} LG_\theta$, and similarly for $H_\nu{}^*$

This is useful for giving a prior assessment of the significance of the induced flow. When estimates are available for the physical parameters the pairs of matrices, for example C and C^*, can be compared for detectable changes in the values of their elements.

Eliminating the vector $\underline{c}$ between A6 and A5 gives

$$\tau\ \underline{\lambda}' + \underline{\lambda} = F_{\beta'}\ \underline{\beta}' + F_{\beta}\ \underline{\beta} + F_{\theta}\ \underline{\theta} + F_{\nu}\ \underline{\nu} + F_{\lambda}\ \underline{\lambda}$$

or

$$\tau\ \underline{\lambda}' + (I - D_{\lambda})\underline{\lambda} = F_{\beta'}\ \underline{\beta}' + F_{\beta}\ \underline{\beta} + F_{\theta}\ \underline{\theta} + F_{\nu}\ \underline{\nu}$$

where $F_{\beta} = LG_{\beta}$ etc.

REFERENCES

1. C.G. Black, "A Methodology for the Identification of Helicopter Mathematical Models from Flight Data Based on the Frequency Domain", Ph.D. Thesis, Dept. of Aerospace Engineering, University of Glasgow, July 1988.
2. C.G. Black, D.J. Murray-Smith and G.D. Padfield, "Experience with Frequency-Domain Methods in Helicopter System Identification" 12th European Rotorcraft Forum, Garmish-Partenkirchen, Fed. Rep. of Germany, September 1986, Paper 76.
3. C.G. Black, "Consideration of Trends in Stability and Control Derivatives from Helicopter System Identification" 13th European Rotorcraft Forum, Arles, France, September 1987, Paper 7.8.
4. G.D. Padfield, "A Theoretical Model of Helicopter Flight Mechanics for Application to Piloted Simulation", RAE TR 81048, April 1981.
5. R.A. Ormiston and D.A. Peters, "Hingeless Helicopter Rotor Response with Non-uniform Inflow and Elastic Blade Bending" J. Aircraft, Vol. 9, No. 10, 1972.
6. W. Johnson, "Helicopter Theory" Princetown University Press, 1980.
7. R.W. Du Val, O. Bruhis and J.A. Green, "Derivation of a coupled Flapping/Inflow Model for the Puma Helicopter" HTP-6 System Identification Workshop RAE Bedford, 1988.

ACKNOWLEDGEMENTS

The authors would like to acknowledge the contribution of Dr. G.D. Padfield of the Royal Aerospace Establishment, Bedford to this work. This research was carried out as part of the Ministry of Defence Extra Mural Agreement 2048/46/XR/STR as a contribution to the HTP-6 System Identification Workshop, Bedford, 1988 under the auspices of The Technical Cooperation Programme.

Parameter*	Equation-Error Estimate 0.213-1.60 Hz	Equation-Error Estimate 0.035-1.60 Hz.	Output-Error Estimate 0.213-1.60 Hz.	Approx. Theoretical
a_{21}	-6.498 (0.692)+	-9.6	-7.611 (0.89)	-6.776
a_{22}	-5.249 (0.52)	-2.5	-10.69 (0.76)	-10.898
a_{23}	-3.318 (0.88)	-7.1	-5.71 (0.66)	-4.587
b_{22}	-5.542 (0.63)		-13.06 (1.4)	-10.810
b_{23}	23.37 (0.83)		28.9 (1.9)	27.5
b_{21}	1.951 (1.74)		-10.54 (3.8)	5.261
	R^2 = 0.9916		Cost Value = -1365.3	

* quantities are not normalised by rotor frequency Ω

+ estimated 1 σ error bounds

TABLE 1. Estimates of significant parameters (non-physical) in the model:

$$\begin{bmatrix} \beta_o \\ \beta_{1c} \\ \beta_{1s} \end{bmatrix}' = \begin{bmatrix} a_{11} & a_{12} & a_{13} \\ a_{21} & a_{22} & a_{23} \\ a_{31} & a_{32} & a_{33} \end{bmatrix} \begin{bmatrix} \beta_o \\ \beta_{1c} \\ \beta_{1s} \end{bmatrix}$$

$$+ \begin{bmatrix} b_{11} & b_{12} & 0 & 0 & b_{15} & b_{16} & 0 \\ b_{21} & b_{22} & b_{23} & 0 & 0 & 0 & b_{27} \\ b_{31} & b_{32} & b_{34} & 0 & b_{35} & b_{36} & b_{37} \end{bmatrix} \begin{bmatrix} \theta_{1cw} \\ \theta_{1sw} \\ \overline{q}_w \\ \overline{p}_w \\ q'_w \\ p'_w \\ \theta_o \end{bmatrix} + \begin{bmatrix} K_1 \\ K_2 \\ K_3 \end{bmatrix}$$

Parameter	Output-Error Estimate 0.226 - 1.581 Hz	Approximate Theoretical
$1 - \lambda_\beta{}^2$ ⇓	-0.5488 (0.060)†	-
$\lambda_\beta{}^2$	1.5488	1.06
n_β	1.0311 (0.060)†	0.987

† Estimated 1σ error bound

TABLE 2. Estimates of physical parameters (no induced-flow dynamics).

Parameter	Momentum-Inflow Output-Error Estimate 0.226 - 1.581 Hz	Vortex-Inflow Output-Error Estimate 0.226 - 1.581 Hz	Approximate Theoretical
$1 - \lambda_\beta{}^2$ ⇓	-0.5276 (0.063)†	-0.6509 (0.074)†	-
$\lambda_\beta{}^2$	1.5276	1.6509	1.06
n_β	1.1149 (0.075)†	1.2912 (0.079)†	0.987
τ	-8.23± (5.0)†	-0.287± (3.3)†	-

† Estimated 1σ error bound

± Normalised by Ω ($\Omega \triangleq 27.5$ rad s^{-1})

TABLE 3. Estimates of physical parameters (with induced flow dynamics)

Parameter	Estimates for First-Order Model Without Inflow	Estimates for First-Order Model With (Momentum) Inflow Model	Approximate Theoretical
a_{21}	-7.214	-6.347	-6.776
a_{22}	-13.944	-13.713	-10.896
a_{23}	0.329	0.330	-4.587
b_{22}	-11.141	-11.039	-10.810
b_{23}	27.5(fixed)	27.5(fixed)	27.5
b_{21}	5.698	5.518	5.261

TABLE 4. Estimates of parameters in the model of Table 1. (Values constructed from estimates of physical parameters λ_β and n_β).

FIGURE 1 a): MEASURED AND PREDICTED FREQUENCY-DOMAIN MAGNITUDES FOR THE FIRST-ORDER MODEL WITH NO INFLOW.

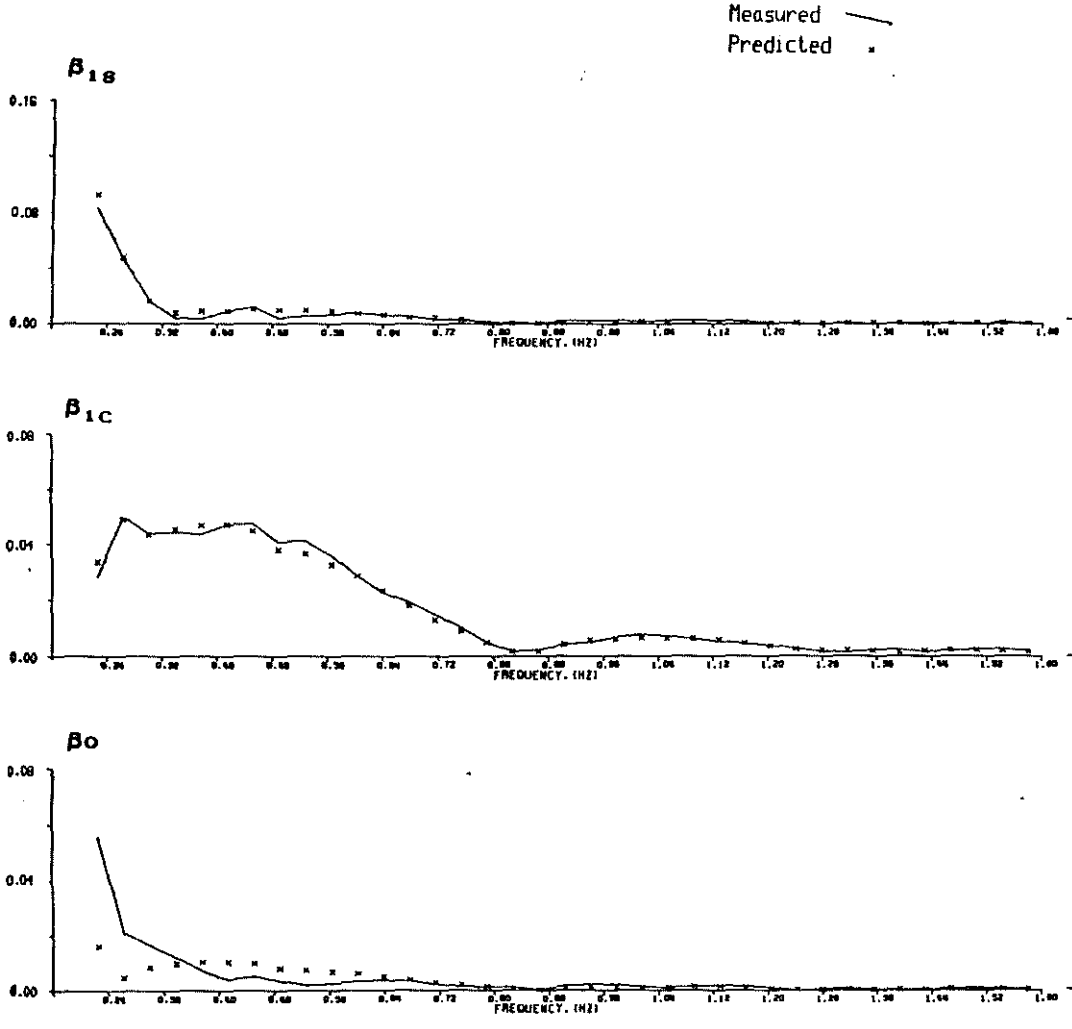

FIGURE 1 b): MEASURED AND PREDICTED PHASE-ANGLE VALUES FOR THE FIRST-ORDER MODEL WITH NO INFLOW.

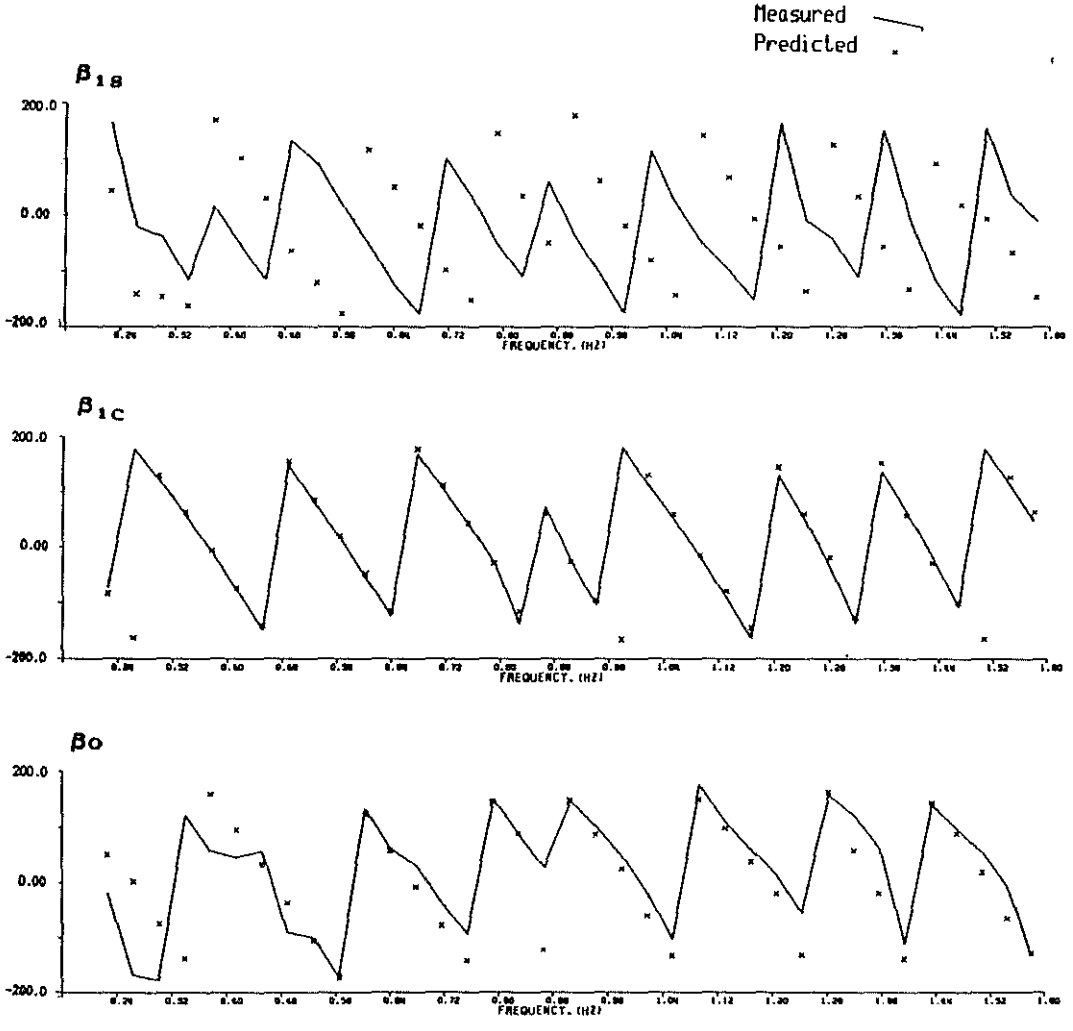

FIGURE 2 a): MEASURED AND PREDICTED FREQUENCY-DOMAIN MAGNITUDES FOR THE FIRST-ORDER MODEL WITH INFLOW MODELLED USING MOMENTUM THEORY.

FIGURE 2 b): MEASURED AND PREDICTED PHASE-ANGLE VALUES FOR THE FIRST-ORDER MODEL WITH INFLOW MODELLED USING MOMENTUM THEORY.

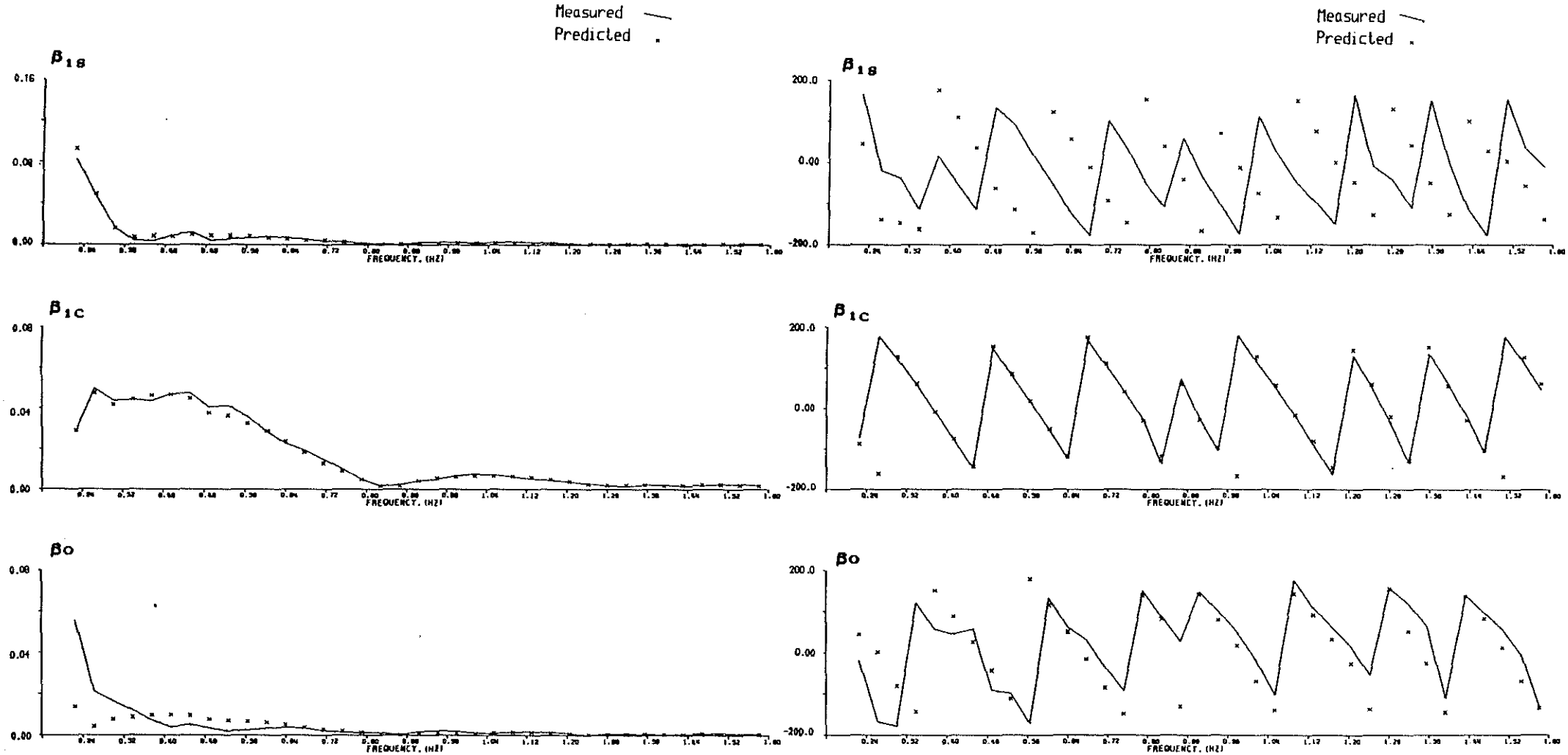

FIGURE 3: TIME-DOMAIN RECONSTRUCTIONS OF FREQUENCY-DOMAIN IDENTIFIED MODEL WITH INFLOW MODELLED USING MOMENTUM THEORY.